

Low-temperature magneto-thermal transport investigation of a Ni-based superconductor BaNi_2As_2 : Evidence for fully gapped superconductivity

N. Kurita¹, F. Ronning¹, Y. Tokiwa¹, E. D. Bauer¹, A. Subedi^{2,3}, D. J. Singh², J. D. Thompson¹, and R. Movshovich¹

¹*Los Alamos National Laboratory, Los Alamos, New Mexico 87545, USA*

²*Materials Science and Technology Division, Oak Ridge National Laboratory, Oak Ridge, Tennessee 37831-6114, USA*

³*Department of Physics and Astronomy, University of Tennessee, Knoxville, Tennessee 37996-1200, USA*

(Dated: March 5, 2009)

We have performed low-temperature specific heat and thermal conductivity measurements of the Ni-based superconductor BaNi_2As_2 ($T_c = 0.7$ K) in magnetic field. In zero field, thermal conductivity shows T -linear behavior in the normal state and exhibits a BCS-like exponential decrease below T_c . The field dependence of the residual thermal conductivity extrapolated to zero temperature is indicative of a fully gapped superconductor. This conclusion is supported by the analysis of the specific heat data, which are well fit by the BCS temperature dependence from T_c down to the lowest temperature of 0.1 K.

PACS numbers: 74.70.Dd, 74.25.Fy, 74.25.Op

Since the discovery of superconductivity in $\text{LaFeAs}(\text{O},\text{F})$ [1], there has been considerable interest in the oxy-pnictide $RT\text{Pn}(\text{O},\text{F})$ and the related structure $AT_2\text{Pn}_2$ ($R = \text{La, Ce, Sm, Nd}$, $A = \text{Ca, Ba, Sr, Eu}$, $T = \text{Fe, Ni}$, $\text{Pn} = \text{P, As}$) due to (i) their high superconducting temperature T_c (up to 55 K for $\text{SmFeAs}(\text{O},\text{F})$ [2] and 38 K for $(\text{Ba},\text{K})\text{Fe}_2\text{As}_2$ [3]), (ii) their proximity to magnetism, and (iii) the large variety in structure and composition that supports superconductivity. Ni-based materials differ from their Fe-based cousins in that (i) long-range magnetic order has not yet been observed in close proximity to superconductivity, although similar structural transitions are found, and (ii) T_c does not exceed 5 K in any of the Ni-based systems, although for virtually every structural variant where the Fe system superconducts, so too does the Ni analog. Substitution of Ni for Fe modifies a number of properties that may be responsible for suppression of T_c . Identifying the commonalities and, especially, the differences between the compound in the two families, will in turn provide clues into why T_c in Fe-based superconductors is so high.

One important issue to resolve with any new superconductor is to identify the superconducting order parameter as that may shed light into the pairing mechanism. Comparing the character of the superconducting gap in Ni- and Fe-based systems present an ideal opportunity to elucidate the pairing mechanism responsible for the relatively high T_c in Fe-based compounds. In the iron-based oxy-pnictides or $A\text{Fe}_2\text{Pn}_2$ compounds, NMR measurements suggest a nodal gap structure [4, 5], which contradicts penetration depth [6], Andreev spectroscopy [7], and angle-resolved photoelectron spectroscopy (ARPES) measurements [8] that indicate a fully gapped multi-band superconductor. To our knowledge, similar measurements that address the character of the superconducting order parameter have not been done on the Ni analogs [9, 10, 11, 12, 13, 14, 15].

We present a study of the gap structure of BaNi_2As_2 using low temperature thermal conductivity and heat capacity. Thermal conductivity, as a bulk probe of low energy delocalized excitations, has proven to be a powerful tool for identifying nodal [16], s -wave [17], and multi-band superconductors [18]. We chose to study BaNi_2As_2 as a representative Ni-based superconductor. Bulk superconductivity in this material at 0.7 K is confirmed by heat capacity measurements, while, similar to many Fe-pnictides, a first order structural transition exists at 130 K [12].

Single crystals of BaNi_2As_2 (ThCr₂Si₂-type tetragonal structure) were grown in Pb flux as described in Ref. 12. Thermal conductivity was measured between 40 mK and 4 K by a standard one-heater and two-thermometers technique on plate-like crystals with dimensions of $\sim 1 \times 0.5 \times 0.1$ mm³ for a heat current $q \parallel [100]$. Specific heat of several single crystals (6.91 mg) were measured by a standard heat pulse method. In the thermal conductivity study, two samples from different batches were measured, which are denoted as #1 and #2. Sample #1 is the same one used in previous resistivity experiments (Ref. 12). Magnetic field was applied within *ab*-plane for $H \perp q$ (#1 and #2) and $H \parallel q$ (#1).

First, we consider the possible superconducting gap symmetry of BaNi_2As_2 based on heat capacity data. Figure 1(a) shows specific heat divided by temperature C/T as a function of T in zero field which supports the notion that BaNi_2As_2 is a weak coupling superconductor. The upturn below 0.2 K is ascribed to a nuclear quadrupolar Schottky anomaly arising mainly from As. The solid line is a fit to $C = C_{\text{BCS}} + C_{\text{Sch}}$, where $C_{\text{Sch}} = A/T^2$ and C_{BCS} is the BCS expression:

$$C_{\text{BCS}} = t \frac{d}{dt} \int_0^\infty dy \left(-\frac{6\gamma\Delta_0}{k_B\pi^2} \right) [f \ln f + (1-f) \ln(1-f)].$$

Here $t = T/T_c$, $f = 1/[\exp(E/k_B T) + 1]$, $E = (\epsilon^2 + \Delta^2)^{1/2}$ and $y = \epsilon/\Delta_0$, as described in Ref. 19. As seen in

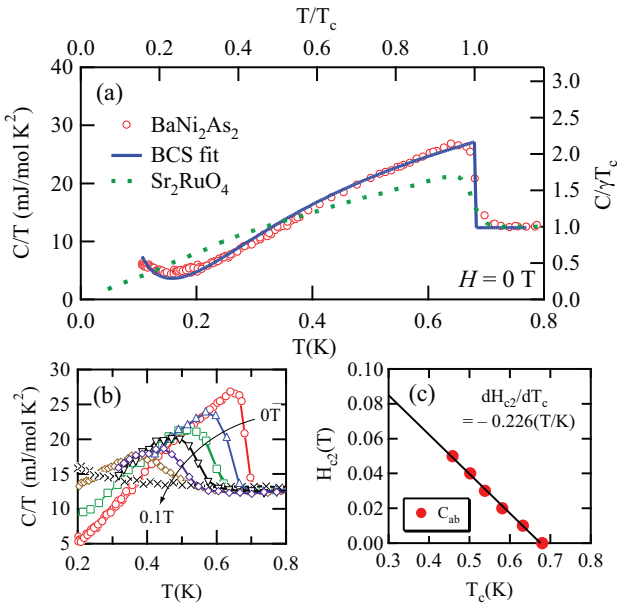


FIG. 1: (Color online) (a) Zero-field low-temperature specific heat, plotted as C/T vs T , of BaNi_2As_2 and Sr_2RuO_4 [21] (with T_c and γT_c scaled to that of BaNi_2As_2) for comparison. The solid curve is a fit to the theoretical expectation for BCS superconductivity including a nuclear quadrupolar Schottky contribution. (b) C/T vs T in fields of 0, 0.01, 0.02, 0.03, 0.04, 0.05 and 0.1 T (right to left as indicated by the arrow) for $H \parallel ab$. (c) Upper critical field H_{c2} for $H \parallel ab$ as determined by the midpoint of the jump in C/T . The solid line represents a least-squares fit to the data.

Fig. 1(a), the specific heat data can be fit over a wide temperature range from just above T_c down to the lowest temperature, yielding a Sommerfeld coefficient $\gamma = 12.3 \text{ mJ/mol K}^2$, $A = 8.6 \times 10^{-3} \text{ mJK/mol}$, equivalent to the energy splitting of the nuclear quadrupolar levels of As of $\nu_Q \approx 30 \text{ MHz}$ [20], and $\Delta_0 = 0.0946 \text{ meV} = 1.61 k_B T_c$ ($T_c = 0.68 \text{ K}$ was fixed during the fit). The reduced magnitude of the energy gap Δ_0 , compared with the expected BCS gap $\Delta_{\text{BCS}} = 0.103 \text{ meV} = 1.76 k_B T_c$ for a weak coupling BCS superconductor, is likely due to the fact that our BaNi_2As_2 samples are in the dirty limit as will be discussed below based on the analysis of thermal conductivity data. In contrast, specific heat of a well established unconventional superconductor Sr_2RuO_4 , also displayed in Fig. 1(a), shows a much slower decrease with temperature, expected for nodal superconductivity [21].

Fig. 1(b) shows the temperature dependence of C/T in several fields for $H \parallel ab$ in BaNi_2As_2 . As field increases, the jump shifts to low temperature region, whereas it becomes broader and less detectable above 0.05 T. The upper critical field H_{c2} , determined by the midpoint of the jump at each field, is displayed in Fig. 1(c). The solid line is a least-squares fit

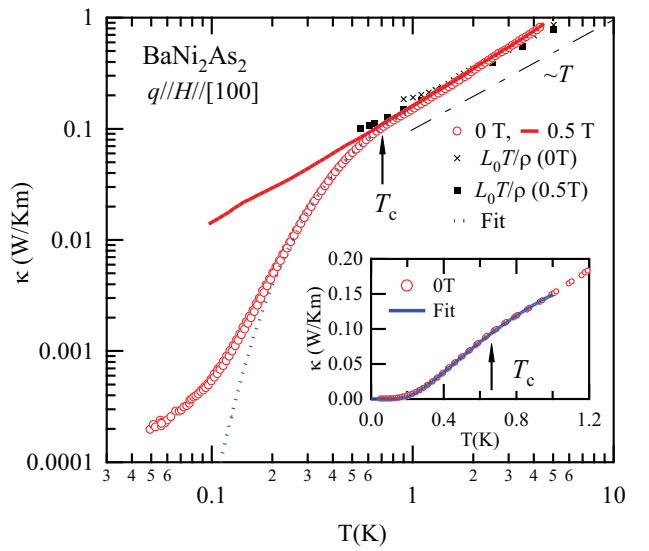


FIG. 2: (Color online) Temperature dependence of the thermal conductivity $\kappa(T)$ in BaNi_2As_2 for heat current $q \parallel [100]$, in zero field and in the normal state (0.5 T) for $H \parallel ab$. Arrows indicate T_c determined from the specific heat measurement. Solid square and cross symbol represent the electronic thermal conductivity $\kappa_e = L_0 T / \rho$ with $L_0 = 2.45 \times 10^{-8} \text{ W}\Omega/\text{K}^2$ for 0 and 0.5 T, respectively, derived from resistivity data using the Wiedemann-Franz law. Dotted line in main figure and solid line in the inset show a fit to $\kappa(T)$ with a BCS curve defined as $\kappa = C \exp(-a T_c / T)$.

to the H_{c2} data, yielding an initial slope $dH_{c2}/dT_c = -0.226 \text{ T/K}$, which results in a zero-temperature upper critical field $H_{c2}(0) = 0.11 \text{ T}$, using the estimate $H_{c2}(0) = -0.7 T_c dH_{c2}/dT_c$ [22]. This yields a Ginzburg-Landau coherence length $\xi = 550 \text{ \AA}$ from the relationship $\xi = (\Phi_0 / 2\pi H_{c2}(0))^{1/2}$, where $\Phi_0 = 2.07 \times 10^{-7} \text{ Oe cm}^2$ is the flux quantum. An estimate of the electronic mean free path l_e is obtained from the normal state thermal conductivity using $\kappa/T = 1/3\gamma v_F l_e$, with a Fermi velocity $v_F = 2.96 \times 10^5 \text{ m/s}$ which was calculated by methods described in Ref. 23. We find $l_e \approx 70 \text{ \AA}$ and $l_e/\xi = 0.13$, which places BaNi_2As_2 in the dirty limit. The field dependence of the residual linear term $\gamma_0 T$ of the heat capacity can be used to identify whether or not the superconducting order parameter has nodes. However, in the low temperature region, especially below 0.2 K, the addenda contribution, as well as the nuclear term, grow with increasing field, making an accurate estimate of $\gamma_0(H)$ difficult. In this regard, thermal conductivity, which is not subject to these effects, is ideally suited for directly determining the low-temperature behavior.

Fig. 2 shows the temperature dependence of thermal conductivity $\kappa(T)$ of BaNi_2As_2 in zero field and 0.5 T ($\gg H_{c2}$) for heat current $q \parallel [100]$. In zero field and in the normal state above $T_c = 0.7 \text{ K}$, $\kappa(T)$ exhibits an approximately T -linear variation, which continues to the lowest

temperature in a field of 0.5 T. Using the Wiedemann-Franz law, we estimate an electronic thermal conductivity in the normal state $\kappa_e = L_0 T / \rho$ in zero-field and 0.5 T where the Lorenz number $L_0 = 2.44 \times 10^{-8} \text{ W}\Omega/\text{K}^2$. As seen in Fig. 2, $\kappa_e(T)$ is very close to $\kappa(T)$ in the normal state, suggesting that heat transport in the normal state is dominated by the electrons. In the superconducting state, $\kappa(T)$ follows an exponential form ($\sim \exp(-aT_c/T)$ with $a = 1.34$) down to 0.2 K as shown in the inset of Fig. 2. This evolution of $\kappa(T)$ in BaNi_2As_2 is quite similar to the conventional superconductors tin, aluminum, and zinc with $T_c = 3.7, 1.2$ and 0.84 K, respectively [24]. The thermal conductivity for these three elements is also described by $\kappa(T) \sim \exp(-aT_c/T)$ with $a = 1.3 - 1.5$ below T_c . In fact, the thermal conductivity based on BCS superconductivity for weak coupling [25] is well-described by the formula $\exp(-aT_c/T)$ with $a = 1.47$. Thus, the a -value of 1.34 for BaNi_2As_2 is in good agreement with that for conventional BCS superconductors. Below 0.2 K, $\kappa(T)$ does not fall as rapidly as expected for an exponential dependence and reaches $2 \times 10^{-4} \text{ W/K m}$ at 50 mK. Similar deviations from an exponential dependence were observed in a number of conventional superconductors, including tin and aluminum [24], and are usually attributed to phonon contribution. When most of the normal quasiparticles are frozen out, the intrinsic electronic thermal conductivity is too low to make an appreciable contribution. In fact, an upper limit of the phonon thermal conductivity estimated via $\kappa_{\text{ph}} = \frac{1}{3} \beta T^3 \langle v \rangle l_{\text{ph}} = 2.0 \times 10^{-4} \text{ W/K m}$, using the phonon specific coefficient $\beta = 18.7 \text{ J/K}^4 \text{ m}^3$, mean phonon velocity $\langle v \rangle = 1860 \text{ m/s}$ [12] and the phonon mean free path $l_{\text{ph}} = 1.38 \times 10^{-4} \text{ m}$ [26], is equal to the experimental value $2 \times 10^{-4} \text{ W/K m}$ at 50 mK in BaNi_2As_2 . Although we cannot rule out other origins of the low temperature tail, agreement between the estimated and the measured values at 50 mK suggests a phonon origin of the low temperature thermal conductivity in BaNi_2As_2 . Note that nuclear quadrupolar moments, while leading to a Schottky term dominating specific heat below 200 mK, do not contribute to thermal conductivity.

The low-temperature magnetic field dependence of κ is instructive for determining the gap structure. Fig. 3 shows the low-temperature expansion of κ/T vs T^2 of BaNi_2As_2 for a heat current $q \parallel [100]$ in several fields for $H \perp q$. The straight lines are fits to $\kappa/T = \kappa_0/T + bT^2$, where κ_0/T is the residual term extrapolated to $T = 0$ K at each field. With increasing field, κ_0/T rapidly increases above 0.02 T and saturates above 0.15 T. This rise could only be attributed to the electron contribution, as the phonon thermal conductivity may only go down in magnetic field due to additional scattering from vortices in the mixed state. The field dependence of the residual thermal conductivity of BaNi_2As_2 is shown in Fig. 4(a) as $(\kappa_0/T)/(\kappa_n/T)$ vs H/H_{c2} for $H \perp q$ (#1). From the thermal conductivity data, $H_{c2} = 0.16$ T is de-

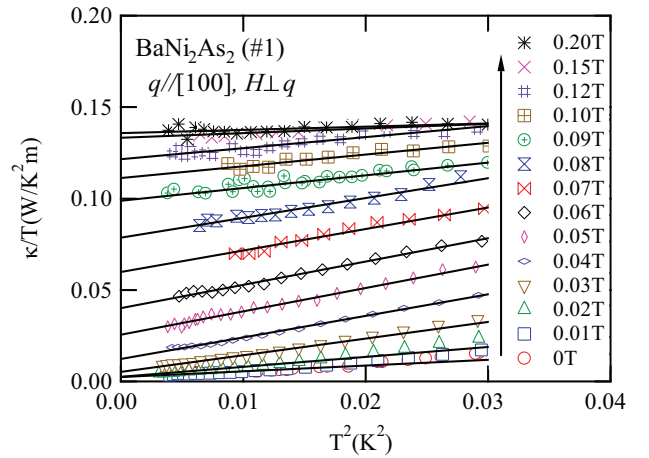


FIG. 3: (Color online) Low-temperature dependence of κ/T vs T^2 for $q \parallel [100]$ in several fields for $H \perp q$. The solid lines are fits to the data in the temperature range by $\kappa/T = \kappa_0/T + bT^2$

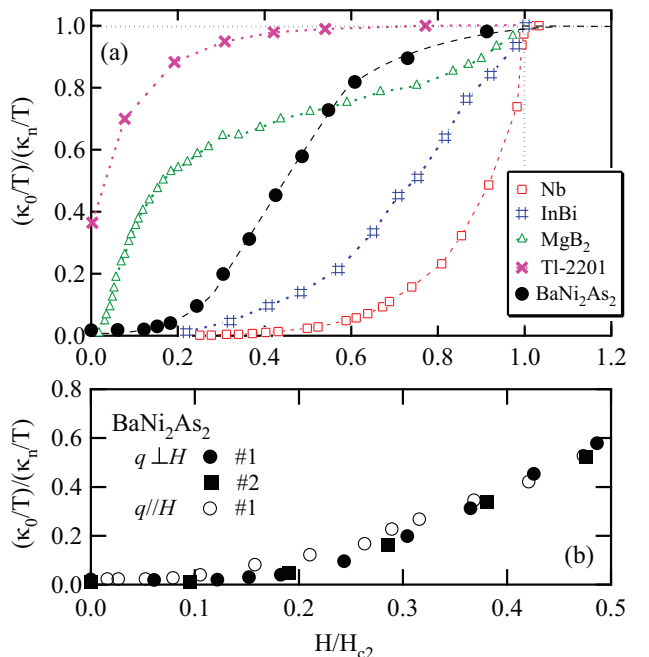


FIG. 4: (Color online) (a) Residual thermal conductivity κ_0/T of BaNi_2As_2 , normalized by the normal state value κ_n/T above H_{c2} , as a function of H/H_{c2} for $H \perp q$ (#1). A small contribution from the Pb flux has been subtracted. For comparison, data for several superconductors with different superconducting gap characteristics are shown: Nb (clean, fully gapped s -wave) [27], InBi (dirty, fully gapped s -wave) [17], MgB₂ (multi-band gap) [18], Tl-2201 (d -wave with line nodes) [16]. The dotted lines are guides to the eyes. (b) $(\kappa_0/T)/(\kappa_n/T)$ vs H/H_{c2} of BaNi_2As_2 for $H \perp q$ (#1, #2) and $H \parallel q$ (#1).

terminated as the field where κ_0/T becomes independent of the magnetic field. κ_n/T at 0.2 T is used as the normal state value. Data for several superconductors with different gap structures are also shown for comparison. The simplest test of *s*-wave superconductivity is whether the residual thermal conductivity exhibits a concave variation with field as vortices begin to penetrate the sample at low fields. The exponential-like concave behavior is understood as follows: when vortices first enter the sample at $H \geq H_{c1}$, quasiparticles that contribute to thermal conductivity are mostly localized around the vortex cores. Therefore, at low field, those quasiparticles cannot carry heat until the intervortex spacing is decreased sufficiently that states created in the vortices begin to overlap, become delocalized, and hence, transport heat, as illustrated by the clean *s*-wave superconductor Nb[27]. In contrast, the presence of nodal quasiparticles leads to a convex field dependence as a consequence of the Volovik effect [28], as illustrated by Tl-2201,[16]. As seen in Fig. 4(b), $(\kappa_0/T)/(\kappa_n/T)$ exhibits concave feature independent of heat current direction with respect to magnetic field, and independent of sample difference. Consequently, *the concave field-dependence of the thermal conductivity implies that BaNi₂As₂ is a fully gapped superconductor*.

The field dependence of $\kappa(H)$ for BaNi₂As₂ more closely resembles the dirty *s*-wave superconductors such as InBi, than the clean case (i.e., Nb), which is consistent with our estimate of $l_e/\xi \ll 1$. In addition, the data appear to display a shoulder-like anomaly at 0.7 H_{c2} , suggesting an additional energy scale at that field. This may reflect a spread in H_{c2} as reflected by the width of the heat capacity anomaly in field. On the other hand, the shoulder might be due to multiband character of superconductivity in BaNi₂As₂, although the anomaly in thermal conductivity is much less dramatic than in MgB₂. And there is no obvious evidence for multiband physics in the heat capacity data of Fig. 1. However, interband scattering would be expected to wipe out multiband effects in our relatively dirty material. Additional studies on cleaner crystals would help to resolve this issue.

For the FeAs-based superconductors, it has been argued that an unconventional superconducting state may still give rise to a fully gapped excitation spectrum if the nodal planes, where the phase of the order parameter changes sign, do not intersect the Fermi surface [29]. Density functional calculations for BaNi₂As₂, however, find a much more complicated Fermi surface for which it is difficult to imagine finding a nodal plane which does not intersect the Fermi surface [23]. Thus, the fully gapped Fermi surface in BaNi₂As₂ is due to the superconducting order parameter that does not change sign. If the superconducting order parameter in FeAs systems does indeed change sign, the pairing mechanism in the FeAs and NiAs systems is likely to be of different origin, as argued by band structure calculations [23, 30].

In conclusion, we have performed magneto-thermal transport experiments to elucidate the superconducting gap symmetry of BaNi₂As₂. The following results indicate that BaNi₂As₂ is a dirty fully gapped superconductor: (i) specific heat data are well-fit by the BCS formula, (ii) the coherence length is much larger than the electronic mean free path, and, (iii) the field dependence of the residual thermal conductivity is consistent with a dirty fully gapped superconductivity.

We would like to thank I. Vekhter M. Graf, S.-H Baek and H. Sakai for useful discussions. Work at Los Alamos National Laboratory was performed under the auspices of the US Department of Energy. Work at Oak Ridge was supported by the DOE, Division of Materials Sciences and Engineering.

[1] Y. Kamihara *et al.*, J. Am. Chem. Soc. **130**, 3296 (2008).
[2] Z.-A. Ren *et al.*, Chin. Phys. Lett. **25**, 2215 (2008).
[3] M. Rotter *et al.*, Phys. Rev. Lett. **101**, 107006 (2008).
[4] Y Nakai *et al.*, J. Phys. Soc. Jpn. **77**, 073701 (2008).
[5] K. Matano *et al.*, Europhys. Lett. **83**, 57001 (2008).
[6] K. Hashimoto *et al.*, Phys. Rev. Lett. **102**, 017002 (2009).
[7] X.H. Chen *et al.*, Nature **453**, 761 (2008).
[8] H. Ding *et al.*, Europhys. Lett. **83**, 47001 (2008).
[9] T. Watanabe *et al.*, Inorg. Chem. **46**, 7719 (2007). T. Watanabe *et al.*, J. Solid State Chem. **181**, 2117 (2008).
[10] T. Mine *et al.*, Solid State Commun. **147**, 111 (2008).
[11] H. Fujii and S. Kasahara, J. Phys.: Condens. Matter **20**, 075202 (2008).
[12] F. Ronning *et al.*, J. Phys.: Condens. Matter **20**, 342203 (2008).
[13] E.D. Bauer *et al.*, Phys. Rev. B **78**, 172504 (2008).
[14] T. Klimczuk *et al.*, Phys. Rev. B **79**, 012505 (2009).
[15] V.L. Kozhevnikov *et al.*, JETP. Lett. **87**, 747 (2008).
[16] C. Proust *et al.*, Phys. Rev. Lett. **89**, 147003 (2002). M. Suzuki *et al.*, Phys. Rev. Lett. **88**, 227004 (2002).
[17] J. Willis and D. Ginsberg, Phys. Rev. B **14**, 1916 (1976). M. Sutherland *et al.*, Phys. Rev. Lett. **98**, 067003 (2007).
[18] A.V. Sologubenko *et al.*, Phys. Rev. B **66**, 014504 (2002). E. Boaknin *et al.*, Phys. Rev. Lett. **90**, 117003 (2003).
[19] See, for example, M. Tinkham, *Introduction to Superconductivity* (McGraw-Hill, New York), (1975).
[20] $\nu_Q \approx 30$ MHz is comparable to values of ν_Q for other compounds of this family. For example, $\nu_Q = 13.93$ MHz for CaFe₂As₂, S.-H. Baek *et al.* arXiv:0808.0744v3. Direct measurements of ν_Q in BaNi₂As₂ via NQR will be useful.
[21] S. Nishizaki *et al.*, J. Low Temp. Phys. **117**, 1581 (1999).
[22] N.R. Werthamer *et al.*, Phys. Rev. **147**, 295 (1966).
[23] A. Subedi and D.J. Singh, Phys. Rev. B **78**, 132511 (2008).
[24] See, for example, R. Berman, *Thermal conduction in Solids* (Oxford Univ. Press, Oxford), (1976) and references therein.
[25] J. Bardeen *et al.*, Phys. Rev. **113**, 982 (1959).
[26] $\Lambda_0 = \frac{2}{\pi} \sqrt{ab}$, where $a = 73 \mu\text{m}$ and $b = 640 \mu\text{m}$ are sample cross section dimensions. A nearly order of magnitude difference between a and b can lead to an overestimate

of l_{ph} . See, M.P. Zaitlin *et al.*, Phys. Rev. **B** **12**, 4487 (1975).

[27] J. Lowell and J.B. Sousa, J. Low. Temp. Phys. **3**, 65 (1970).

[28] G.E. Volovik, JETP Lett. **58**, 469 (1993).

[29] e.g. K. Seo *et al.*, Phys. Rev. Lett. **101**, 206404 (2008).

[30] A. Subedi *et al.*, Phys. Rev. B **78**, 134514 (2008).